Supplementary Information (SI) for Nanoscale Advances.

Synergistic catalytic and antibacterial activity, along with in silico molecular docking of bimetallic silver-copper doped PVP-$Mg(OH)_2$ nanostructures

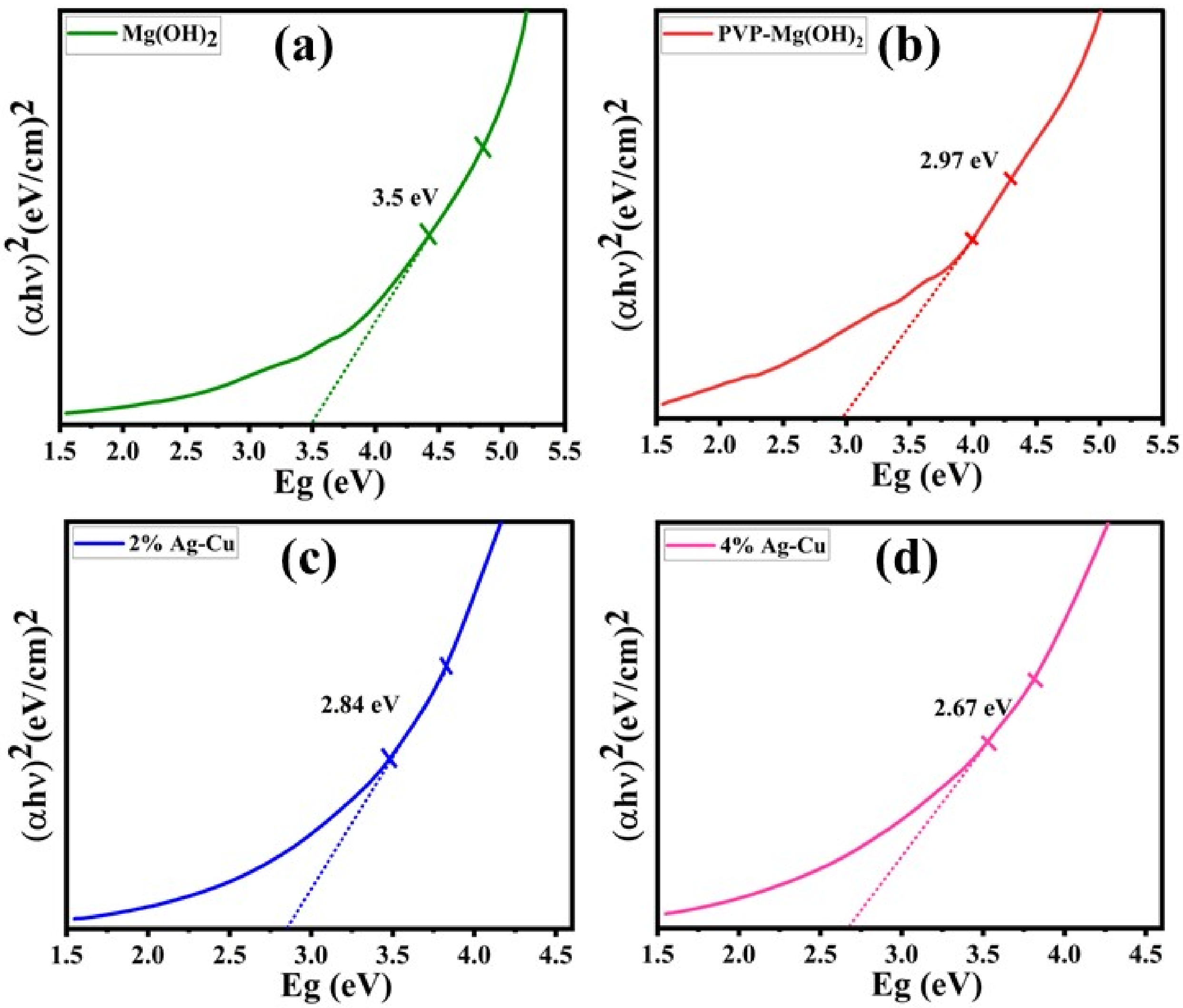

Fig. S1: Tauc plots for Eg of (a) $Mg(OH)_2$, (b) PVP-$Mg(OH)_2$, (c) 2% Ag-Cu/PVP-$Mg(OH)_2$, and, (d) 4% Ag-Cu/PVP-$Mg(OH)_2$ NSs

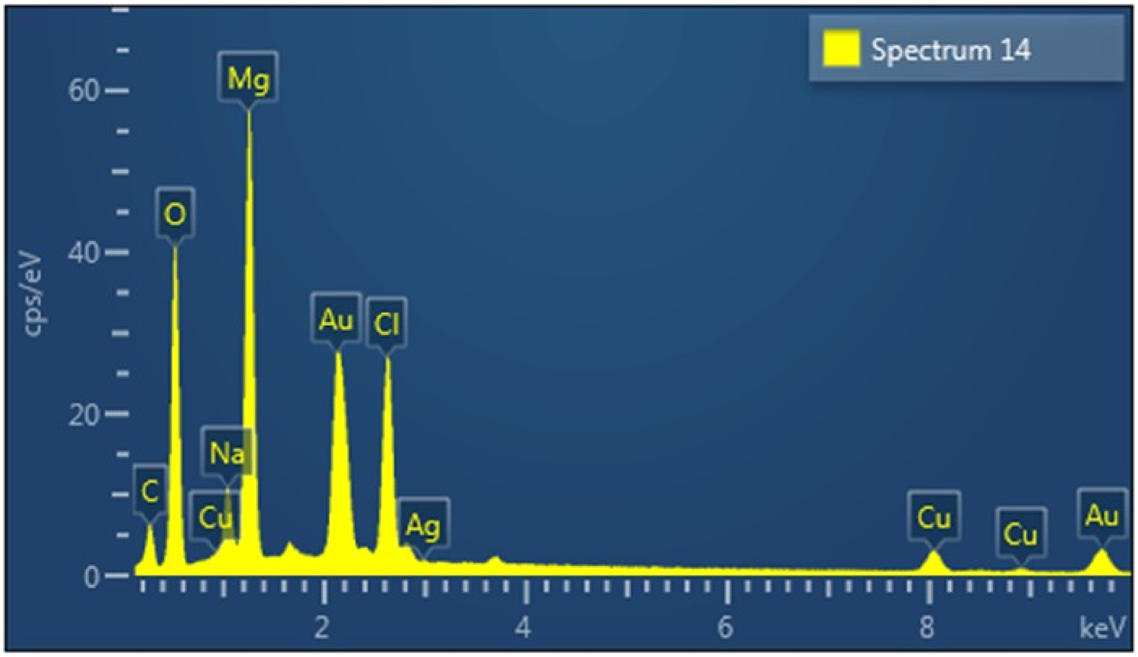

Fig. S2: EDS spectra of 4% Ag-Cu/PVP-$Mg(OH)_2$

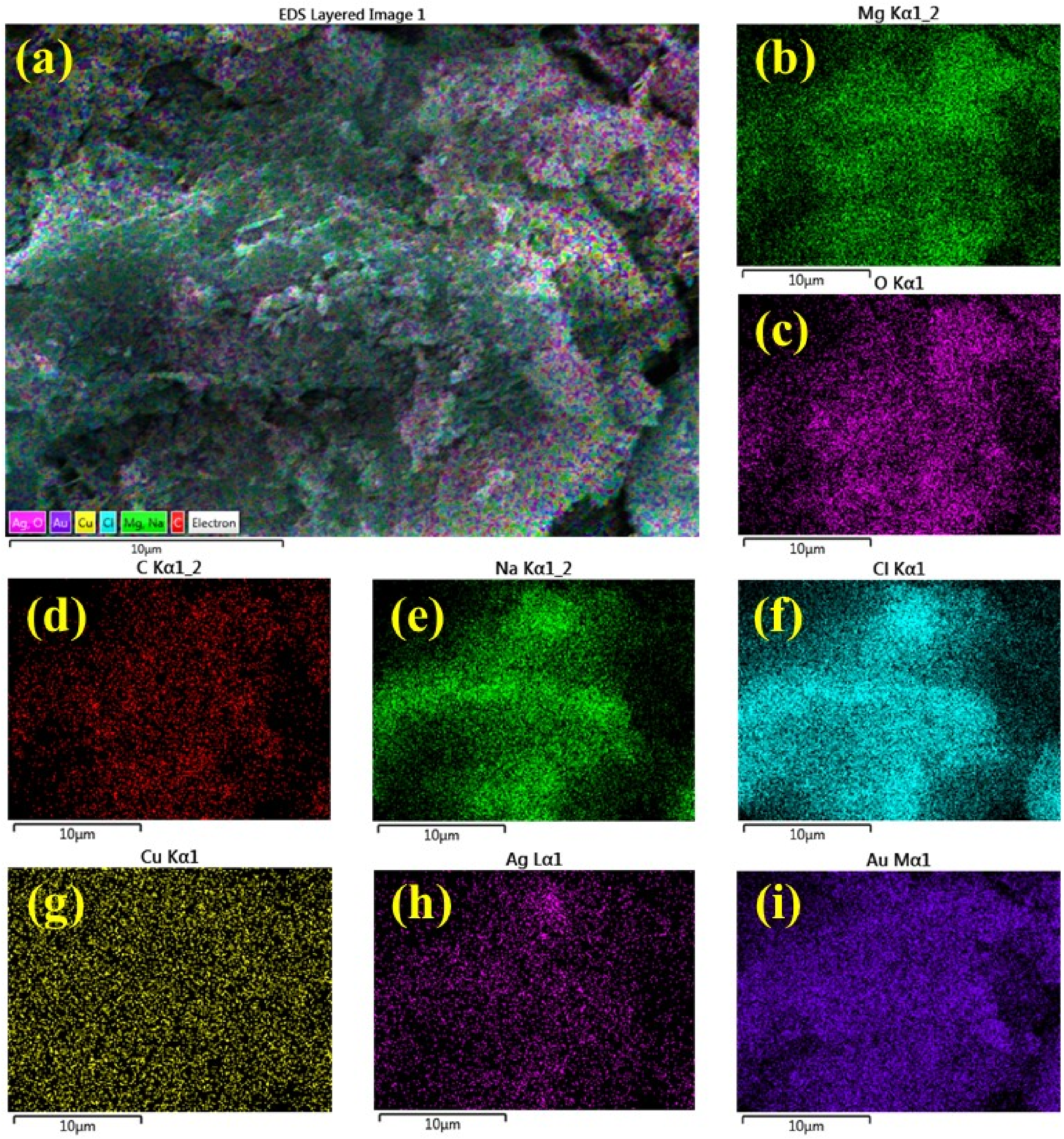

Fig. S3: Mapping of (a) 4% Ag-Cu/PVP-$Mg(OH)_2$, (b) Magnesium (Mg), (c) Oxygen (O), (d) Carbon (C), (e) Sodium (Na), (f) Chlorine (Cl), (g) Copper (Cu), (h) Silver (Ag), and (i) Gold (Au)

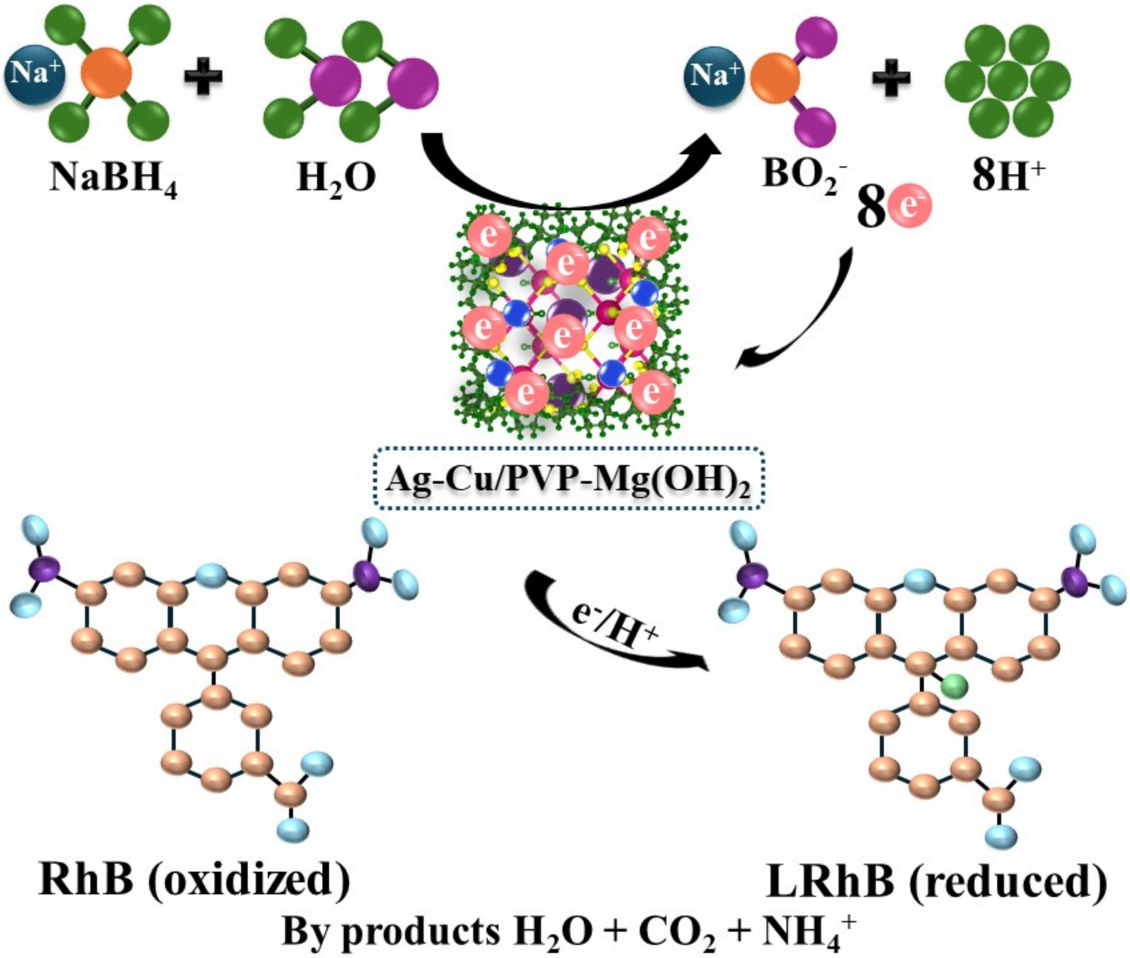

Fig. S4: Catalytic mechanism of Ag-Cu/PVP-$Mg(OH)_2$ NSs

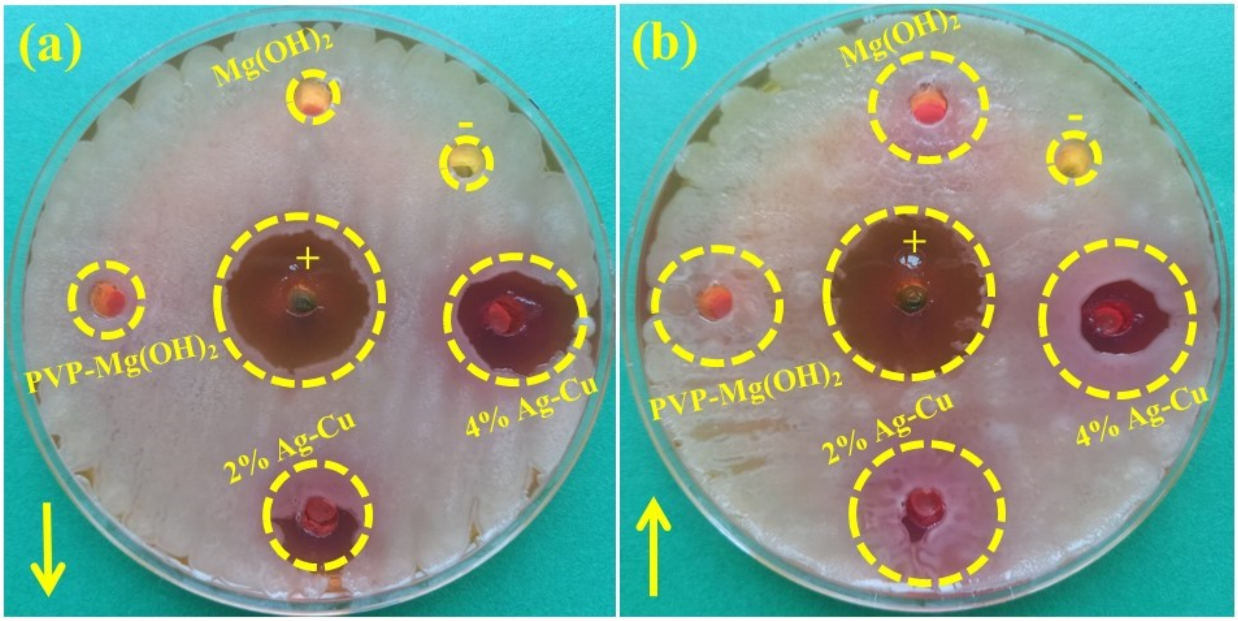

Fig. S5: Inhibition zone of prepared NSs at (a) low, and (b) high concentration

Table S1. Comparison table of present work with literature

Sr. no.	Material	Dye	% Degradation	Time	References
1.	$Mg(OH)_2$	methylene blue	55%	2 h	[1]
2.	$Mg(OH)_2$-PVP	methylene blue	69%	2 h	[1]
3.	$Mg(OH)_2$	methylene blue	98%	60 min	[2]
4.	Fe_3O_4/PVP/PS	AR18	94.4%	45 min	[3]
5.	PVP-capped ZnS	methylene blue	81%	6 h	[4]
6.	$FePMo_{12}O_{40}$@PVP	RhB	83%	40 min	[5]
7.	Ag-Cu doped TiO_2	MO	50%	40 min	[6]

8.	Fe3O4@TiO2/Ag, Cu	RhB	86.19%	30 min	[7]
9.	Ag-Cu@ZnO	RhB	94%	-	[8]
10.	$g\text{-}C_3N_4/Ag/Cu_2O$	RhB	85%	50 min	[9]
11.	Ag-Cu/PVP-$Mg(OH)_2$	RhB	99.68%	10 min	Present study

Table S2. Comparison table of antibacterial efficacy of Ag-Cu/PVP-$Mg(OH)_2$ with literature

Sr. no.	Material	Bacteria	Efficacy %age	Reference
1.	$Mg(OH)_2$	*S. aureus*	35.5 %	[10]
2.	$Mg(OH)_2$	*E. coli*	85 %	[1]
3.	PVP-BaO	*S. aureus*	38.15 %	[11]
4.	PVP-ZnO	*B. subtilis*	80 %	[12]
5.	Cu0.5Ag0.5 doped HA600	*S. aureus*	50.1 %	[13]
6.	Ag-Cu/PVP-$Mg(OH)_2$	*S.aureus*	94.1 %	Present study

Table S3. Surflex score of docked ligands bonded to DNA gyrase molecular targets.

Protein	**Docked Ligands**	**CScore** [a]	**Crash score**[b]	**Polar score**[c]	**G score**[d]	**PMF score**[e]	**D score**[f]	**Chem score**[g]
DNA Gyrase*S. aureus*	PVP-$Mg(OH)_2$	4.39	-0.58	5.31	-61.609	26.088	-380.442	-4.320

	Ag-Cu/PVP-$Mg(OH)_2$	6.21	-1.37	6.00	-77.068	37.471	-841.199	-4. 124
	Ciprofloxacin	5.98	-1.98	2.85	-172.945	-3.595	-99.729	-12.366

[a]**CScore** is consensus scoring method that ranks ligand affinity using different scoring algorithms.
[b]**Crash-score** indicates binding site interference**.**
[c]Ligand **polarity**,
[d]**G-score** explains hydrogen bonding energies, ligand-protein interactions, and ligand internal energies.
[e]**PMF-score** represents Helmholtz free energies associated with protein-ligand atom pairs (Potential of Mean Force, PMF).
[f]**D-score** represents protein-ligand charge and van der Waals interactions.
[g]**Chem-score** emphasizes hydrogen bonding, lipophilic interactions, and rotational entropy

1. Dharamalingam, K., et al., *Facile synthesis of polymer-based magnesium hydroxide nanocomposites for photocatalytic degradation for methylene blue dye and antibacterial application.* Biomass Conversion and Biorefinery, 2023. **13**(15): p. 13539-13552.
2. Das, P.S., et al., *Unique microstructure of 3D self-assembled Mg (OH) 2 nanoparticles for methylene blue degradation in presence of direct sun light.* Transactions of the Indian Ceramic Society, 2018. **77**(4): p. 226-234.
3. Elbarbary, A.M., et al., *Synthesis and characterization of magnetically retrievable Fe3O4/polyvinylpyrrolidone/polystyrene nanocomposite catalyst for efficient catalytic oxidation degradation of dyes pollutants.* Journal of Inorganic and Organometallic Polymers and Materials, 2022. **32**(2): p. 383-398.
4. Soltani, N., et al., *Photocatalytic degradation of methylene blue under visible light using PVP-capped ZnS and CdS nanoparticles.* Solar Energy, 2013. **97**: p. 147-154.

5. Wang, Z., et al., *Polymer-Based Immobilized FePMo12O40@ PVP Composite Materials for Photocatalytic RhB Degradation.* Inorganics, 2024. **12**(6): p. 144.

6. Jalali, J., M. Mozammel, and M. OjaghiIlkhchi, *Photodegradation of organic dye using co-doped Ag/Cu TiO 2 nanoparticles: synthesis and characterization.* Journal of Materials Science: Materials in Electronics, 2017. **28**: p. 16776-16787.

7. Ghafuri, H., et al., *Synthesis and characterization of magnetic nanocomposite Fe3O4@ TiO2/Ag, Cu and investigation of photocatalytic activity by degradation of rhodamine B (RhB) under visible light irradiation.* Optik, 2019. **179**: p. 646-653.

8. Gangarapu, M., et al., *Highly recyclable and ultra-rapid catalytic reduction of organic pollutants on Ag–Cu@ ZnO bimetal nanocomposite synthesized via green technology.* Applied Nanoscience, 2018. **8**: p. 1123-1131.

9. Liang, S., et al., *Preparation of porous g-C3N4/Ag/Cu2O: a new composite with enhanced visible-light photocatalytic activity.* Applied Organometallic Chemistry, 2016. **30**(11): p. 932-938.

10. Dhaouadi, H., H. Chaabane, and F. Touati, *Mg (OH) 2 nanorods synthesized by a facile hydrothermal method in the presence of CTAB.* Nano-Micro Letters, 2011. **3**(3): p. 153-159.

11. Ikram, M., et al., *Antibacterial potential with evidential molecular docking analysis and catalytic performance of multiple phases AgBr and PVP doped BaO nanorods.* Journal of Molecular Structure, 2025. **1328**: p. 141371.

12. Singh, K., et al., *Light-absorption-driven photocatalysis and antimicrobial potential of PVP-capped zinc oxide nanoparticles.* Scientific Reports, 2023. **13**(1): p. 13886.

13. Kamonwannasit, S., et al., *Synthesis of copper-silver doped hydroxyapatite via ultrasonic coupled sol-gel techniques: structural and antibacterial studies.* Journal of Sol-Gel Science and Technology, 2020. **96**: p. 452-463.